Prediction of Veneer Moisture Content Based on Near Infrared Spectroscopy

Kang Zhou, Yutang Chen, Chengshuo Sun, and Bin Na *

The physical properties of wood, particularly the dimensional stability, are affected by the water content. Most wood properties can be detected by near infrared spectroscopy (NIRS), which is used as a nondestructive testing method. At different wavelengths, different absorption peaks are presented with the moisture absorbed by wood. According to this feature, the absorption peaks can be collected, and the data can be processed by partial least squares method combined with NIRS. In this study, softwood oak and hardwood ash tree specimens were studied. In the infrared spectrum range, the wood moisture absorption curve was noticeable and the curve trend was similar, although the tree species were different. After centralization, standardization, and derivative processing of the spectral data, the correlation coefficients of oak and ash tree validations were high, reaching 0.9021 and 0.9661, respectively. The wood moisture content was predicted using NIRS and an algorithm. The experiments showed that this method is feasible.

DOI: 10.15376/biores.17.4.5878-5889

Keywords: Moisture content; Near infrared spectroscopy; Algorithm; Physical properties

Contact information: Nanjing Forestry University, Nanjing 210037 China;
** Corresponding author: nabin8691@126.com*

INTRODUCTION

The size of wood is affected by the moisture content (Daassi-Gnaba *et al.* 2017; Ramage *et al.* 2017). Keplinger *et al.* (2015) found that there was a large amount of water in the wood cell cavity and cell wall, and the moisture content was affected by the drying effect. Under the influence of air humidity, drying shrinkage and swelling were generated when a non-ideal drying method was carried out (Li and Li 2000; Remik *et al.* 2012; Chen *et al.* 2016; Gao *et al.* 2016; Liu *et al.* 2016). Wood cracking and deformation were caused by these phenomena.

In the process of using wood, the wood moisture content is usually controlled in a lower range, and the instability of the wood size is affected by the moisture content (Liu and Wang 2004; Na *et al.* 2011; Wang and Chen 2013; Lu *et al.* 2017). The quality problems of wood and its derivatives are mostly caused by the inaccuracy of moisture content detection and control in wood processing. Therefore, it is important to monitor the wood moisture content in real time to extend wood products' service life (Dai and Ahmet 2001; Tamme *et al.* 2013; Brischke and Lampen 2014). Due to the widespread use of logging and the depletion of forest resources, stricter cutting and processing methods have been necessary. Therefore, wood processing efficiency can be promoted and the quality of wood products can be improved with the real-time nondestructive and accurate measurement of wood moisture content (Jones *et al.* 2005; Li *et al.* 2009; Mai *et al.* 2015).

There are many techniques to determine the wood moisture content, such as the traditional drying method according to the GB/T-1931 (2009) standard for the determination of the wood moisture content. Relatively accurate measurement results can be obtained, but this method cannot meet the requirements of a real-time measurement. The distillation method is suitable for the detection of wood moisture content that contains more volatile components. However, with the distillation method, the test material microstructure is destroyed and the measurement time is long. Currently, the resistance method is widely used in the wood industry to detect the moisture content (Stamm 1927; Moss *et al.* 2009). The advantages of the resistance method are simple detection steps, a low cost, and data time-effectiveness. However, the applicable moisture content of the resistance method is only 6% to 30%, and the measurement results are affected by temperature to a certain extent. Voltage needs to be applied to the sample for resistance data, and the structure of the sample may be destroyed thereby (Bakraji *et al.* 2002; Li *et al.* 2019).

Near infrared spectroscopy (NIRS) is a new detection technology with the advantages of a short corresponding time, a high measurement accuracy, and non-destructive testing (Schimleck *et al.* 2002; Kelley *et al.* 2004; Heman and Hsieh 2016; Clavaud *et al.* 2017; Wang *et al.* 2020). Near infrared refers to the electromagnetic wave with wavelengths in the range of 780 to 2,526 nm. It is produced by the non-resonance of molecular vibration when molecular vibration changes from ground state to high energy level. A large amount of hydroxyl groups are found in wood, which are hydrophilic. The polarity of water molecules is very strong. In addition, water molecules have strong absorption in infrared when they vibrate, which makes it convenient for NIRS to study the structure and chemical composition of water molecules. Three obvious absorption peaks were observed at 1,145, 1,450, and 1,940 nm in the water absorption spectrum. Based on this, the spectral information in this wavelength range has been widely used to study water conditions.

Wood moisture content can be predicted by partial least squares combined with NIRS. Spectral data were gathered, and a water content prediction model was established after centralization, standardization, first-order derivative treatment, and second-order derivative treatment (Xu *et al.* 2005; Qin and Mo 2006; Wang and Shen 2009). This method was feasible through experimental analysis, which provided a simple, fast, and nondestructive method for wood moisture content detection in the processing industry in the future.

EXPERIMENTAL

Materials

The oak (*Quercus spinosa* David ex Franch) and ash tree (*Fraxinus mandshurica* Rupr.) veneer strands were from obtained from Sheng Xiang Wood Floor Co., Zhengjiang, China. A total of 60 pieces of wood were numbered in turn. The specimens with dimensions of 30 mm long × 6 mm wide × 3 mm in height were sawn for the next experiments. One third of the samples were used as validation sets and two thirds of the samples were used as calibration sets.

Control and Determination of the Moisture Content

Firstly, the test sample was placed in an oven until all the moisture was evaporated. The temperature was maintained at 103±2 ℃ during this period. Then, the sample was immersed in water for 12 h until it was nearly completely saturated. Finally, the test sample was dried slowly (temperature: 80 °C, wind velocity: 1m/s, humidity:50%) and the quality was measured continuously in the electric hot air dryer. The data were gathered by NIRS as the sample moisture content reached 60.2% and 40.1%.

Spectral Acquisition

The sample data were gathered by an NIRez spectrometer (Isuzu Optics, Zhubei City, Taiwan). The laboratory temperature and relative humidity were held constant at 26 °C and 20%, respectively. The instrument spectral wavelength range was 960 to 2,150 nm, the integration time was 1 ms, there were 500 scanning times, and the smoothness was five. In the whole infrared spectrum acquisition process, the number of samples is 100 and the moisture contents ranging from 30.2% to 120%.

Data Processing

The model was established though combining the partial least squares method and the principal component analysis. Then, centralization, standardization, first-order derivative, and second-order derivative were processed. It can be observed from the results that the calibration standard error and root mean square error are small, and the prediction model is ideal.

RESULTS AND DISCUSSION

NIRS Characteristics of Samples with Different Moisture Contents

Figure 1 shows the NIRS of two oak samples with different moisture contents. The horizontal coordinate represents the wavelength, and the longitudinal coordinate represents the absorption intensity of the sample to the spectrum.

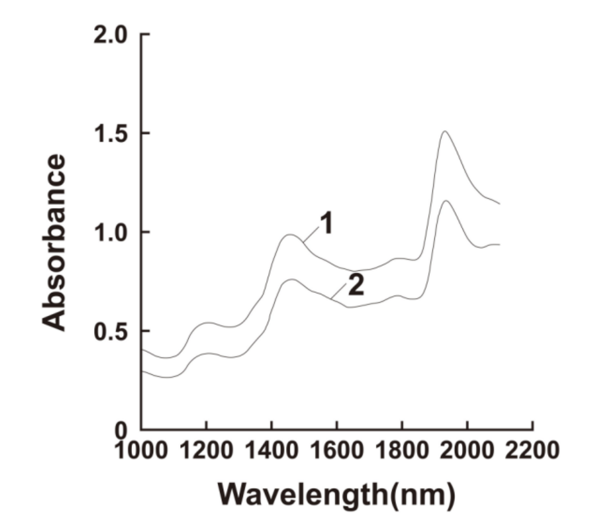

Fig. 1. The NIRS graph of samples with different moisture contents

Curves one and two represent the spectra of the oak samples with moisture contents of 60.2% and 40.1%, respectively. Infrared spectral curves with the same general trend were seen in the same species. Absorbance peak bands were observed at 960, 1,145, 1,450, and 1,950 nm, and relatively obvious absorbance peaks was seen at 1,450 and 1,950 nm. Similar results already had been obtained in 2020 (Zhou *et al.* 2020). However, the peaks they studied were at 1200 and 1460 nm, which were related to the second overtone of the C-H stretching vibration in cellulose or lignin and the first overtone of O-H stretching in cellulose, hemicellulose, and water (Mehrotra *et al.* 2010). The absorbance peak intensity enhanced as the moisture content increased. Wood is composed of cellulose, hemicellulose, and lignin. Mass hydroxyl groups were found in these components, so water can be absorbed by wood due to the hydrophilic chemical bond of O-H.

NIRS Characteristics of the Tree Species

Figures 2 and 3 represent the original diffuse reflection spectrum of 100 oak and ash tree with moisture contents ranging from 30.2% to 120%, respectively. A similar infrared spectrum curve was seen between the oak and ash tree specimens. Absorbance peaks were observed at wavelengths of approximately 1,145, 1,450, and 1,950 nm. The variation in these absorbance peaks was related to the variation in the wood moisture content.

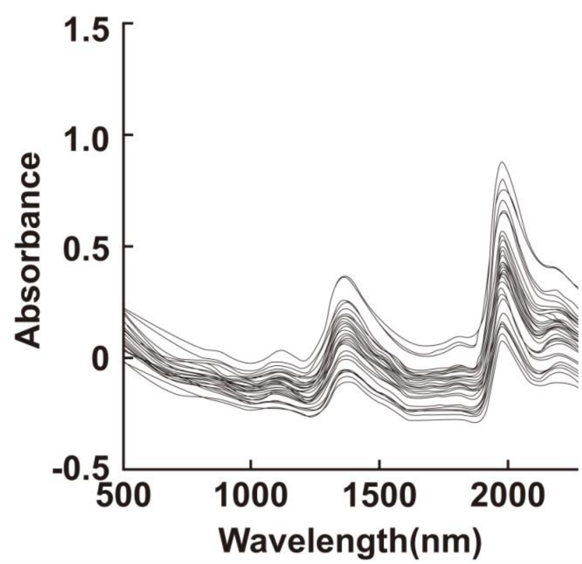

Fig. 2. Original diffuse reflection spectrum of the oak samples

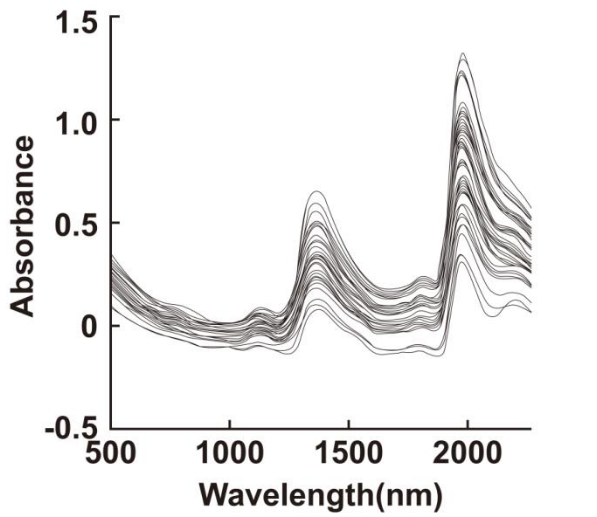

Fig. 3. Original diffuse reflection spectrum of the ash tree samples

Water absorbance peaks mainly occur due to changes in the free water content in capillaries because different water levels can modify the NIR spectrum when incident light is spread on the surface of the specimen.

According to Shi and Feng (2002), a higher or lower spectral range has no significant influence on moisture prediction, the range contained encompasses water absorbance peaks. In this paper, the spectral range from 960 nm to 2,150 nm was selected, and similar results were observed in the range of 800 nm to 2,500 nm.

Prediction of Single Tree Species

Figures 4 and 5 showed the NIRS graphs of the oak samples treated by first-order derivative and second-order derivative, respectively. After the first-order singular derivative treatment and second-order derivative treatment, the spectral absorbance characteristics were more obvious.

The absorbance peaks in the original spectrum can also be presented in the processed spectrum after the first derivative and the second derivative treatment. A relatively better model effect was observed after the first derivative treatment compared to the second derivative treatment, because the environmental interference was eliminated after derivative treatment and the spectral characteristics improved.

The spectral information processed by the first derivative was more obvious than the information that was processed by the second derivative. After the second derivative processing, relatively small information change was highlighted, which may have affected the model results. Most of the effective spectra were located in the wavelength range of 1,000 to 2,100 nm. The general spectral information was found in other bands, so the modeling effect was better in this region.

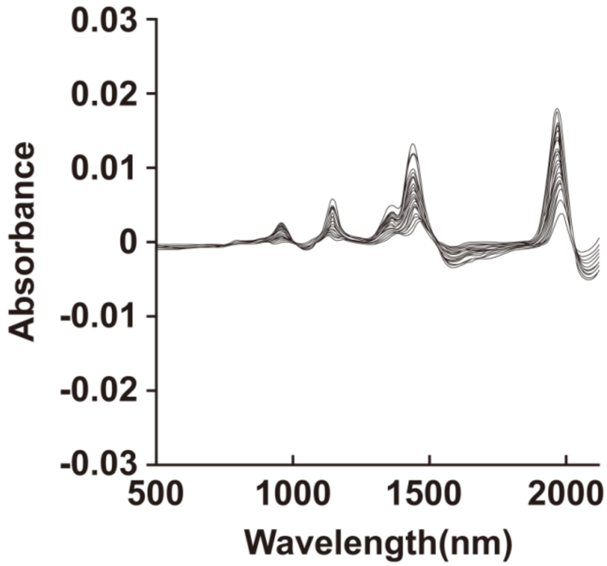

Fig. 4. The NIRS graph of oak after the first derivative treatment

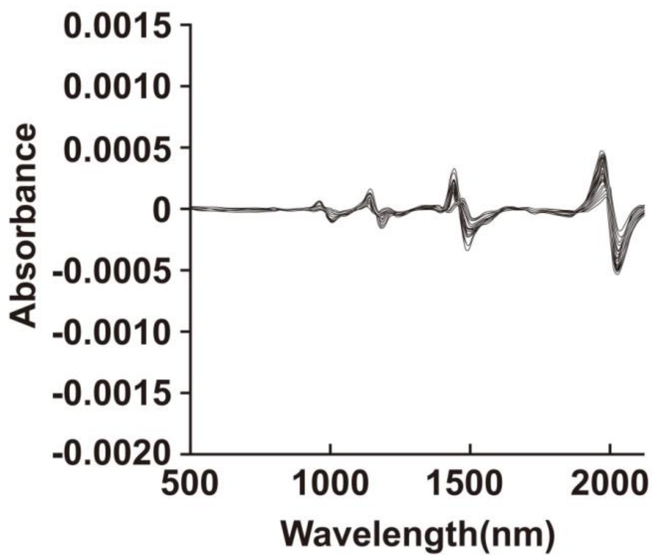

Fig. 5. The NIRS graph of oak after the second derivative treatment

Table 1. Prediction of Oak Moisture Content by Different Pretreatment Methods

Tree Species	Pretreatment Method	Factors Number	RMSEC	Correlation Coefficient of Correction set	Root Mean Square Error of Validation Set	Verification Set Correlation Coefficient
Oak	Original spectrum	8	0.0825	0.8731	0.1472	0.5281
	Original spectrum + centralization + standardization	6	0.0529	0.8973	0.0624	0.8231
	Original spectrum + centralization + standardization + first derivative	7	0.0267	0.9721	0.0597	0.8799
	Original spectrum + centralization + standardization + second derivative	7	0.0121	0.9910	0.0417	0.9021

Table 2. Prediction of Ash Tree Moisture Content by Different Pretreatment Methods

Tree Species	Pretreatment Method	Factors Number	RMSEC	Correlation Coefficient of Correction Set	Root Mean Square Error of Validation Set	Verification Set Correlation Coefficient
Ash tree	Original spectrum	6	0.0801	0.8522	0.2021	0.5481
	Original spectrum + centralization + standardization	5	0.0731	0.8661	0.1792	0.8021
	Original spectrum + centralization + standardization + first derivative	3	0.0501	0.9372	0.0630	0.9327
	Original spectrum + centralization + standardization + second derivative	3	0.0288	0.9771	0.0504	0.9661

Tables 1 and 2 represent the data for the oak and ash tree samples, respectively, under different treatments. The correlation coefficients of the validation sets for the oak and ash tree samples were 0.5281 and 0.5481, respectively. The prediction results of the increase in accuracy were obtained after the model was established by using the spectra after mean centralization and standardization. The correlation coefficients of the validation set for the oak and ash tree samples were 0.8231 and 0.8021, respectively, and the root mean square errors of the validation sets were 0.0624 and 0.1792, respectively. Therefore, the comprehensive performance of the NIRS model can be optimized after centralization and standardization. In addition, the first-order derivative and the second-order derivative of the centralized and standardized spectra were processed respectively, and the accuracy of the established model was further improved. Among them, after centralization, standardization, and second derivative treatment, the best oak model prediction effect was obtained with the model established by the NIRS, and the correlation coefficient of the calibration set of 0.9910 and the correlation coefficient of the validation set of 0.9021. The same result was also existed in the ash tree. The factor number of the ash tree model was 3, and the correlation coefficient of the validation set was 0.9661. Therefore, the quality of the model was directly affected by different pretreatment methods, and the accuracy of model prediction results can be effectively improved with derivative processing.

Prediction of Mixed Tree Species

The mixed tree species moisture content prediction model was established with 60 oak samples and 60 ash tree samples. The calibration set accounted for two thirds, including 40 oak samples and 40 ash tree samples. The validation set accounted for one third, including 20 oak samples and 20 ash tree samples. The mixed tree species prediction model results are shown in Table 3.

Table 3. Prediction of Moisture Content of Oak and Ash Tree by Different Pretreatment Methods

Pretreatment Method	Factors Number	RMSEC	Correlation Coefficient of Correction Set	Root Mean Square Error of Validation Set	Verification Set Correlation Coefficient
Original spectrum	8	0.0873	0.8217	0.1651	0.6927
Original spectrum + centralization + standardization	4	0.0821	0.8556	0.0921	0.8624
Original spectrum + centralization + standardization + first derivative	6	0.0721	0.9112	0.0803	0.9132
Original spectrum + centralization + standardization + second derivative	4	0.0377	0.9721	0.0657	0.9545

Four preprocessing methods that were used in the single prediction model were also used in the mixed prediction model. The data showed that the effect of using the original spectrum to establish the mixed tree model was still poor. There were eight factors, the correlation coefficient of the validation set was only 0.6927, and the root mean square error of the validation set was 0.1651.

The root mean square error was 0.0921, which decreased by 44.2%. In addition, the correlation coefficient of the model validation set that was established by NIRS after centralization, standardization, and first-order derivation was 0.9132, and the root mean square error was 0.0803. However, the correlation coefficient of the model validation set based on NIRS processed by centralization, standardization, and second derivative was 0.9545, and the root mean square error was 0.0657. As the results showed, the wood moisture content prediction model was established with near-infrared spectral data collected from different tree species. The model performance improved greatly when proper original spectrum pretreatment was conducted. The linear fitting results of models with different pretreatment methods are shown in Figs. 6 through 9. The highest model correlation coefficient was observed with the centralization, standardization, and second derivative processing, which had the best linear fitting.

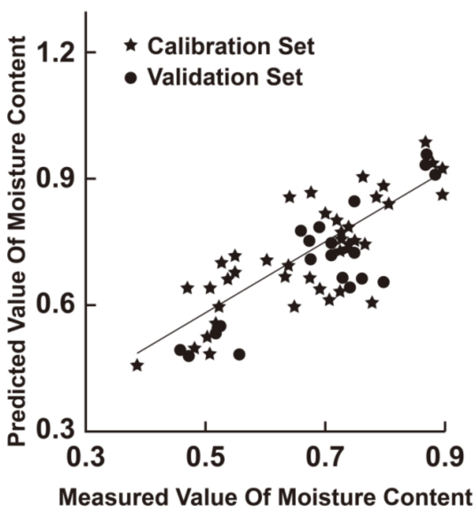

Fig. 6. Original spectrum

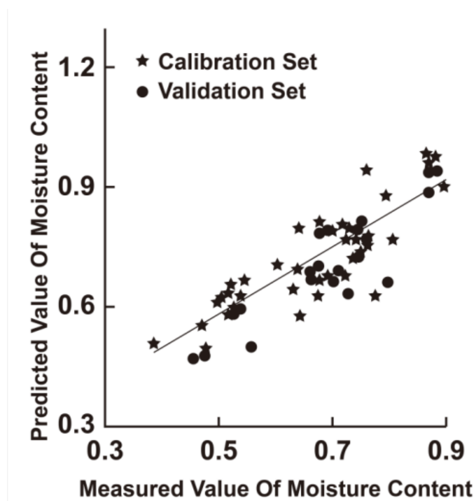

Fig. 7. Original spectrum + centralization + standardization

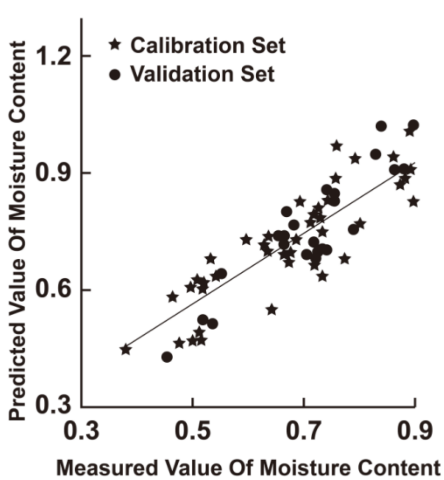

Fig. 8. Original spectrum + centralization + standardization + first derivative

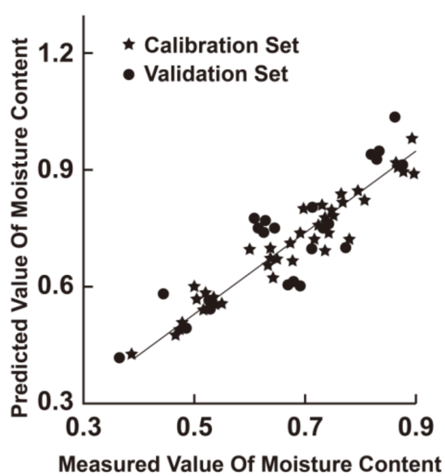

Fig. 9. Original spectrum + centralization + standardization + second derivative

CONCLUSIONS

1. Single and mixed tree species moisture content prediction models can be established by near infrared spectrometry (NIRS) combined with the partial least squares method. The correlation coefficient of the validation set was above 0.9 after centralization, standardization, and derivative treatment.
2. The accuracy of the model prediction results can be effectively improved by spectrum pretreatment. As oak was used to build models, the best prediction effect was obtained after the model was treated with centralization, standardization, and second derivative, and the correlation coefficient of validation set was 0.9021. Under the same model processing method, the correlation coefficient of the validation set of ash tree reached 0.9661. The best effect can also be observed under the same model processing method. In the mixed tree species prediction model, the best prediction effect was obtained after the model was treated with centralization, standardization, and second derivative, and the correlation coefficient of validation set was 0.9545.
3. After correlation, standardization, and second-order derivative treatment, the correlation coefficients of the mixed tree prediction model were not significantly different from those of the single tree prediction model.

ACKNOWLEDGMENTS

This research is supported by the Postgraduate Research & Practice Innovation Program of Jiangsu Province SJCX22_0317. This study was funded by the National Natural Science Foundation (31070502) and the Public Farewell Project of National Forestry Bureau (201004006-6). The authors are also thankful for the support of the Priority Academic Program Development of Jiangsu Higher Education Institutions and the Co-Innovation Center of Efficient Processing and Utilization of Forest Resources, Nanjing Forestry University, Nanjing 210037, China.

REFERENCES CITED

Bakraji, E. H., Salman, N., and Othman, I. (2002). "Radiation-induced polymerization of acrylamide within Okoume (*Aucoumea klaineana* Pierre)," *Radiation Physics and Chemistry* 64(4), 277-281. DOI: 10.1016/S0969-806X(01)00579-5

Brischke, C., and Lampen, S. C. (2014). "Resistance based moisture content measurements on native, modified and preservative treated wood," *European Journal of Wood and Wood Products* 72(2), 289-292. DOI: 10.1007/s00107-013-0775-3

Chen, X., Li, X., Huang, Q., Sun, H., Li, Y., Xie, J., and Xiong, X. (2016). "Characteristics of moisture content and stress changes during the curing period of wood after drying," *Journal of Forestry Engineering* 1(2), 38-43. DOI: 10.13360/j.issn.2096-1359.2016.02.007

Clavaud, M., Roggo, Y., Dégardin, K., Sacré, P.-Y., Hubert, P., and Ziemons, E. (2017). "Global regression model for moisture content determination using near-infrared spectroscopy," *European Journal of Pharmaceutics and Biopharmaceutics* 119, 343-325. DOI: 10.1016/j.ejpb.2017.07.007

Daassi-Gnaba, H., Oussar, Y., Merlan, M., Ditchi, T., Géron, E., and Holé, S. (2017). "Wood moisture content prediction using feature selection techniques and a kernel method," *Neurocomputing* 237, 79-91. DOI: 10.1016/j.neucom.2016.09.005

Dai, G., and Ahmet, K. (2001). "Long-term monitoring of timber moisture content below the fiber saturation point using wood resistance sensors," *Forest Products Journal* 51(5), 52-58.

Feng, X. L, and Shi, Y. G. (2000). "Near infrared spectroscopy and its application in petroleum products," *Institute of Chemistry, Chinese Academy of Sciences ; Chinese Chemical Society*. DOI: 10.14159/j.cnki.0441-3776.2000.03.013

Gao, X., Huang, S., Yuan, Q., and Zhuang, S. (2016). "Research on the drying characteristics of *Dracontomelon duperreranum* and processing," *Journal of Forestry Engineering* 26(2), 108-110.

GB/T 1931 (2009). "Method for determination of the moisture content of wood," Standardization Administration of China, Beijing, China.

Heman, A., and Hsieh, C.-L. (2016). "Measurement of moisture content for rough rice by visible and near-infrared (NIR) spectroscopy," *Engineering in Agriculture, Environment and Food* 9(3), 280-290. DOI: 10.1016/j.eaef.2016.02.002

Jones, P. D., Schimleck, L. R., Peter, G. F., Daniels, R. F., and Clark III, A. (2005). "Nondestructive estimation of *Pinus taeda* L. wood properties for samples from a wide range of sites in Georgia," *Canadian Journal of Forest Research* 35, 85-92. DOI: 10.1139/X04-160

Kelley, S. S., Rials, T. G., Snell, R., Groom, L. H., and Sluiter, A. (2004). "Use of near infrared spectroscopy to measure the chemical and mechanical properties of solid wood," *Wood Sci. Technol.* 38(4), 257-276. DOI: 10.1007/s00226-003-0213-5

Keplinger, T., Cabane, E., Chanana, M., Hass, P., Merk, V., Gierlinger, N., and Burgert, I. (2015). "A versatile strategy for grafting polymers to wood cell walls," *Acta Biomateriala* 11, 256-263. DOI: 10.1016/j.actbio.2014.09.016

Li, D., and Li, Q. (2000). "Study on the drying technology of African rosewood," *China Forest Products Industry* 27(3), 19-21. DOI: 10.19531/j.issn1001-5299.2000.03.005

Li, R., Wang, C., and Liu, C. (2019). "Study on the effects of drying process on microstructure of sweetgum wood," *China Forest Products Industry* 46(7), 23-26. DOI: 10.19531/j.issn1001-5299.201907005

Li, X., and Xu, M. (2009). "Applied research on moisture content measurement: One sided capacitance sensors," *Measurement and Control* 42(3), 84-86. DOI: 10.1177/002029400904200306

Liu, J., and Wang, Y. (2004). "Dimensional stability analysis of poplar and fir treated with phenolic resin," *Chinese Journal of Wood Science and Technology* 6, 5-8. DOI: 10.19455/j.mcgy.2004.06.002

Liu, Y., Lu, C., Su, Y., Wang, J., Lan, J., and Chen, J. (2016). "Drying characteristics of *Eucalyptus macrophylla*," *Eucalyptus Technology* 33(2), 34-43. DOI: 10.13987/j.cnki.askj.2016.02.008

Lu, Q.-j., Li, J.-n., Li, M., Jiang, H.-c., Li, X.-w., and Qin, S.-s. (2017). "Effect of resin concentration on dimensional stability and surface hardness of impregnated rubber wood," *J. Northwest For. Univ.* 32(6), 259-263. DOI: 10.19455/j.mcgy.2004.06.002

Mai, T. C., Razafindratsima, S., Sbartaï, Z. M., Demontoux, F., and Bos, F. (2015). "Non-destructive evaluation of moisture content of wood material at GPR frequency," *Construction and Building Materials* 77, 213-217. DOI: 10.1016/j.conbuildmat.2014.12.030

Mehrotra, R., Singh, P., and Kandpal, H. (2010). "Near infrared spectroscopic investigation of the thermal degradation of wood," *Thermochimica Acta* 507-508, 60-65. DOI: 10.1016/j.tca.2010.05.001

Moss, P. J., Buchanan, A. H., Fragiacomo, M., Lau, P. H., and Chuo, T. (2009). "Fire performance of bolted connections in laminated veneer lumber," *Fire and Materials* 33(5), 223-243. DOI: 10.1002/fam.999

Na, B., Wang, Z., Wang, W., Lu, X., and Wang, Z. (2011). "Two methods to improve the dimensional stability of fast-growing poplar," *Journal of Central South University of Forestry & Technology* 31(8), 183-186. DOI: 10.14067/j.cnki.1673-923x.2011.08.008

Qin, D., and Mo, H. (2006). "Application of artificial neural networks in wood defect detection," *Forest Engineering* 22(1), 21-23. DOI: 10.16270/j.cnki.slgc.2006.01.008

Ramage, M. H., Burridge, H., Busse-Wicher, M., Fereday, G., Reynolds, T., Shah, D. U., Wu, G., Yu, L., Fleming, P., Densley-Tingley, D., *et al*. (2017). "The wood from the trees: The use of timber in construction," *Renew. Sustain. Energy Rev.* 68, 333-359. DOI: 10.1016/j.rser.2016.09.107

Remik, B., Abahri, K., Tahlaiti, M., and Belarbi, R. (2012). "Hygrothermal transfer in wood drying under the atmospheric pressure gradient international," *International Journal of Thermal Sciences* 57, 135-141. DOI: 10.1016/j.ijthermalsci.2012.02.005

Schimleck, L. R., Evans, R., Ilic, J., and Matheson, A. C. (2002). "Estimation of wood stiffness of increment cores by near-infrared spectroscopy," *Canadian Journal of Forest Research* 32, 129-135. DOI: 10.1139/x01-176

Shi, Y. G., Feng, X. L., and Li, Z. C. (2000). "Application of near infrared spectroscopy in testing and evaluation of petroleum products," *Chemistry* 3, 01-02. DOI: 10.14159/j.cnki.0441-3776.2000.03.013

Stamm, A. J. (1927). "The electrical resistance of wood as a measure of its moisture content," *Indust. Engineering Chem.* 19, 1021-1025. DOI: 10.1021/ie50213a022

Tamme, V., Muiste, P., and Tamme, H. (2013). "Experimental study of resistance type wood moisture sensors for monitoring wood drying process above fibre saturation point," *Forestry Studies* 59, 28-44. DOI: 10.2478/fsmu-2013-0009

Wang, R., Wang, X., Jia, R., Gan, J., Ren, H., and Wang, Y. (2020). "Feasibility study on rapid prediction of cork wood density by near-infrared spectroscopy," *Chinese Journal of Wood Science and Technology* 34(5), 54-58. DOI: 10.19455/j.mcgy.20200512

Wang, X., and Shen, S.-j. (2009). "Advances in non-destructive testing for lumber," *Journal of Beijing Forestry University* 31(S1), 202-205.

Wang, Y., and Chen, Z. (2013). "Research on dimensional stability of treated Chinese fir," *Hunan Forestry Science & Technology* 5, 41-44.

Xu, Z., Wang, H., Ding, J., and Yening. (2005). "Defect recognition of log CT images based on artificial neural network," *Chinese Journal of Wood Science and Technology* 4, 15-17. DOI: 10.19455/j.mcgy.2005.04.005

Zhou, Z., Rahimi, S., and Avramidis, S. (2010). "Species- and moisture-based sorting of green timber mix with near infrared spectroscopy," *Chemistry Bioresource* 15, 317-0310. DOI: 10.15376/biores.15.1.317-330

Article submitted: May 28, 2022; Peer review completed: July 23, 2022; Revised version received and accepted: August 2, 2022; Published: August 26, 2022.
DOI: 10.15376/biores.17.4.5878-5889